

# BASIC EQUATIONS FOR THE NEXT GENERATION OF SURFACE TESTERS FOR THE CASE OF AN ELASTIC INDENTER AND A LAYERED SAMPLE

SOLVING THE PROBLEM OF PILE-UP, SINK-IN AND MAKING AREA-FUNCTION-CALIBRATION OBSOLETE BY USING MULTI-AXIAL INDENTATION

Norbert Schwarzer, Saxonian Institute of Surface Mechanics, Tankow 1, 18569 Ummanz, Germany, E-Mail [n.schwarzer@siomec.de](mailto:n.schwarzer@siomec.de), Internet [www.siomec.de](http://www.siomec.de), Tel. ++49(0)1733667359

## ABSTRACT

In the present paper the formulae for the stiffnesses of a new and more general surface tester concept will be given and discussed. Closed form formulae are provided for the case of an elastic indenter on a homogenous half space. It is also shown how an extension to layered materials can be obtained and how the complete elastic fields can be evaluated. The new concept is based on the idea that the next generation of surface testers will provide the means to use all degrees of freedom of movement a probe on a sample surface can perform. Thus, in addition to the ordinary normal stiffness, lateral, tilting stiffness will be measured as well as twisting stiffness and then used in the subsequent parameter determination of the investigated materials. One could call this extension of the ordinary indentation technique a “multi-axial indentation”. It is shown in the paper that such concept would not only solve classical problems like “pile-up” and “sink-in” completely, but it would also supersede the need of area function calibration for the indenter tips and allow direct measurement of local intrinsic and residual stresses, anisotropy and many other things.

## INTRODUCTION

Currently, the great majority of indenter machines is using one axis for indenter movement only, namely in the normal direction<sup>1</sup>. These machines measure independently displacement and load and thus, depend on just one basic equation for the analysis of the sample material. This basic equation is the stiffness of a mechanical contact in normal direction. It gives the result of the derivative of total contact load  $P$  with respect to the displacement or contact depth.

$$\frac{\partial P}{\partial h} = 2aE_r \quad (1)$$

The symbol  $a$  denotes the contact radius and  $E_r$  gives the so called reduced modulus defined as

$$\frac{1}{E_r} = \frac{1-\nu_i^2}{E_i} + \frac{1-\nu_s^2}{E_s}, \quad (2)$$

---

<sup>1</sup> There are currently only very few nanoindenters known to the author (e.g. one prototype as presented in [1] and the UNAT from the company ASMEC) which also provide measurement of load and displacement in lateral direction as accurate as in normal direction. Any reader aware of other such machines should come forward and we will update this footnote.

with  $E_i$ ,  $E_s$  and  $\nu_i$ ,  $\nu_s$  giving the Young's modulus and Poisson's ratio for indenter and sample, respectively.

So, assuming that the material parameters of the indenter are known, there are always three unknowns in the simplest contact situation; the contact radius  $a$ , the sample Young's modulus and the sample Poisson's ratio. While the contact radius can be determined using the "known" indenter geometry calibrated by the means of the so called area function to the contact depth, either of the material parameters  $E_s$  or  $\nu_s$  must be estimated in order to determine the other. Usually it is the Poisson's ratio which is estimated [2]. Unfortunately, the area-function procedure only works well, if the sample material shows a certain deformation behavior, or to put it more accurately, the deformed surface of the sample shows a certain geometry. Deviations from this behavior-assumption, like pile-up or sink in, can lead to significant errors in parameter determination.

In this paper it is therefore demonstrated how the use of additional stiffnesses cannot only overcome these problems, but also open up the way for the extraction of much more material parameters.

## THEORY

For reasons of simplicity and shortness we restrict the following to the case of an elastic homogeneous indenter only. All drawn conclusions are also valid in case of layered indenters and samples, but as the formulae become more complex and lengthy, one requires the help of a computer. Dramatic simplification is possible in the case of a rigid indenter. The interested reader is referred to [3]. The theory presented here is also restricted to symmetry of revolution. This obviously is not a big restriction, because almost all theoretical approaches concerning analyzing techniques for indentation testing are dealing with this simplification. Nevertheless, for high accuracy measurements the author has also developed approaches for the three-sided (Berkowich), the four-sided (Vickers) effective indenter and even asymmetric indenters. The interested reader might want to contact the author directly about this.

We now consider the following additional loads and displacements:

1. Lateral load  $L$  and lateral displacement  $u$
2. Tilting moment  $M$  and tilting angle  $\delta$
3. Twisting Moment  $T$  and twisting angle  $\beta$

As the stiffnesses for other degrees of freedom of probe or indenter movement on the surface of a sample are all defined as derivative of the load with respect to the displacement, we can find the following 6 stiffnesses:

$$S_1 = \frac{\partial P}{\partial h} = 2aE_r \quad (3)$$

$$S_2 = \frac{\partial L}{\partial u} \quad (4)$$

$$S_3 = \frac{\partial L}{\partial \delta} \quad (5)$$

$$S_4 = \frac{\partial M}{\partial u} \quad (6)$$

$$S_5 = \frac{\partial M}{\partial \delta} \quad (7)$$

$$S_6 = \frac{\partial T}{\partial \beta} = \pi a^3 \left( \frac{1+\nu_i}{E_i} + \frac{1+\nu_s}{E_s} \right)^{-1} \quad (8)$$

With  $\vartheta_i = \frac{1}{2} \pi \ln[3-4\nu_i]$ ,  $\vartheta_s = \frac{1}{2} \pi \ln[3-4\nu_s]$  and the following expression:

$$S_2 = a (C3_i C4_i + C3_s C4_s) / (-C2_i (C3_i + C3_s) - C2_s (C3_i + C3_s) + (C1_i + C1_s) (C3_i C4_i + C3_s C4_s))$$

$$S_3 = (a^2 (C2_i + C2_s)) / (-C2_i (C3_i + C3_s) - C2_s (C3_i + C3_s) + (C1_i + C1_s) (C3_i C4_i + C3_s C4_s))$$

$$S_4 = -((a^2 (C3_i + C3_s)) / (C2_i (C3_i + C3_s) + C2_s (C3_i + C3_s) - (C1_i + C1_s) (C3_i C4_i + C3_s C4_s)))$$

$$S_5 = -((a^3 (C1_i + C1_s)) / (C2_i (C3_i + C3_s) + C2_s (C3_i + C3_s) - (C1_i + C1_s) (C3_i C4_i + C3_s C4_s)))$$

$$C1_i = ((1+\nu_i) (\pi \vartheta_i (1+\vartheta_i^2) - (1+4\vartheta_i^2) (-1+\nu_i) \text{Tanh}[\pi \vartheta_i])) / (4 E_i \pi (\vartheta_i + \vartheta_i^3))$$

$$C2_i = (3-3\nu_i-6\nu_i^2) / (8 E_i \pi + 8 E_i \pi \vartheta_i^2)$$

$$C3_i = (3-3\nu_i-6\nu_i^2) / (8 E_i \pi + 8 E_i \pi \vartheta_i^2)$$

$$C4_i = 1/\vartheta_i$$

$$C1_s = ((1+\nu_s) (\pi \vartheta_s (1+\vartheta_s^2) - (1+4\vartheta_s^2) (-1+\nu_s) \text{Tanh}[\pi \vartheta_s])) / (4 E_s \pi (\vartheta_s + \vartheta_s^3))$$

$$C2_s = (3-3\nu_s-6\nu_s^2) / (8 E_s \pi + 8 E_s \pi \vartheta_s^2)$$

$$C3_s = (3-3\nu_s-6\nu_s^2) / (8 E_s \pi + 8 E_s \pi \vartheta_s^2)$$

$$C4_s = 1/\vartheta_s$$

The stiffnesses can be evaluated by using the equations given by Fabrikant [4] and Schwarzer [5]. There it was assumed that in the cases of lateral and twisting movement the measurement of the stiffness can be performed in such a way that only very small displacements occur and the indenter can be modeled as if it was completely bonded. This could easily be achieved by small oscillatory movements also transferring either force or displacement measurement to high accuracy time measurement.

However, it is also possible to evaluate and analyze the situation in cases of higher lateral or twisting displacements usually coming with partially bonded instead of completely bonded indenters as considered for the reason of shortness and simplicity. For these much more complex contact situations we need to distinguish between the (inner) bonded area and an outer region being in contact, but not bonded. Figure 1 shows the resulting indentation behavior caused by this complex contact situation. The red ellipse in Figure 1 marks an area where the resulting nonlinear lateral force to lateral displacement behavior can be seen pretty well. In the case of a completely bonded indenter, which suddenly starts to slide everywhere along the

contact area at a certain lateral load, there would be a straight line within this ellipse. Figure 2 shows the resulting stress in the direction of lateral indenter traction (here the x-axis) for this mixed contact situation at some point within the ellipse-area of figure 1. Only by taking this two-fold contact area into account, the complete lateral loading situation can be theoretically understood and modeled (figure 3).

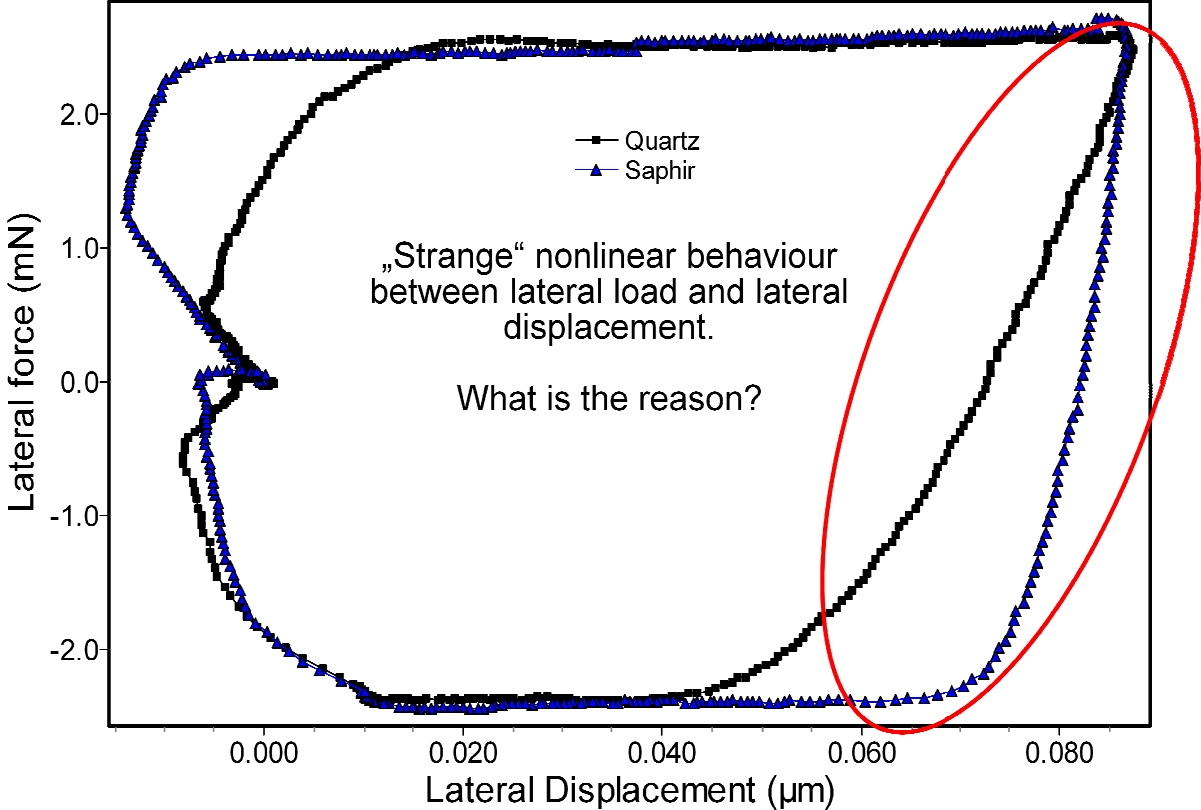


Figure 1: UNAT measurement with a lateral force unit. While the lateral force was running in a circle after the maximum normal load has been reached, the normal load was kept constant. The measurement was performed by T. Chudoba from the company ASMEC.

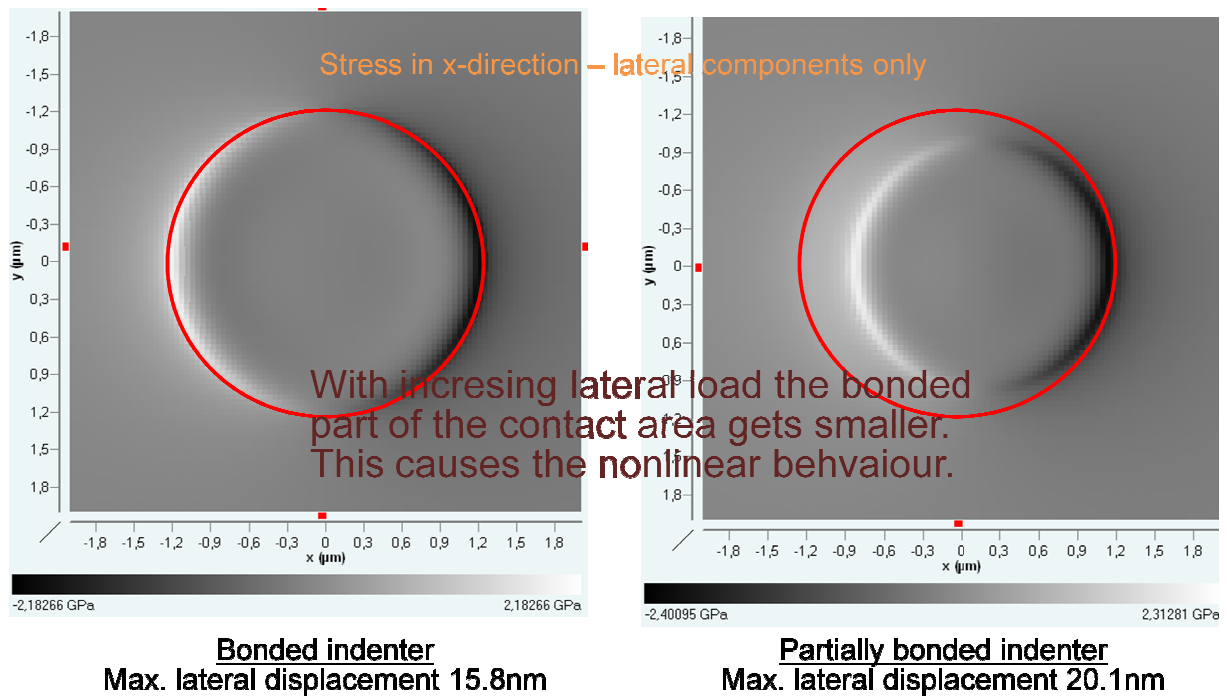


Figure 2: FilmDoctor®-evaluation [6] of the mixed contact-situation resulting in the nonlinear behavior shown in figure 1.

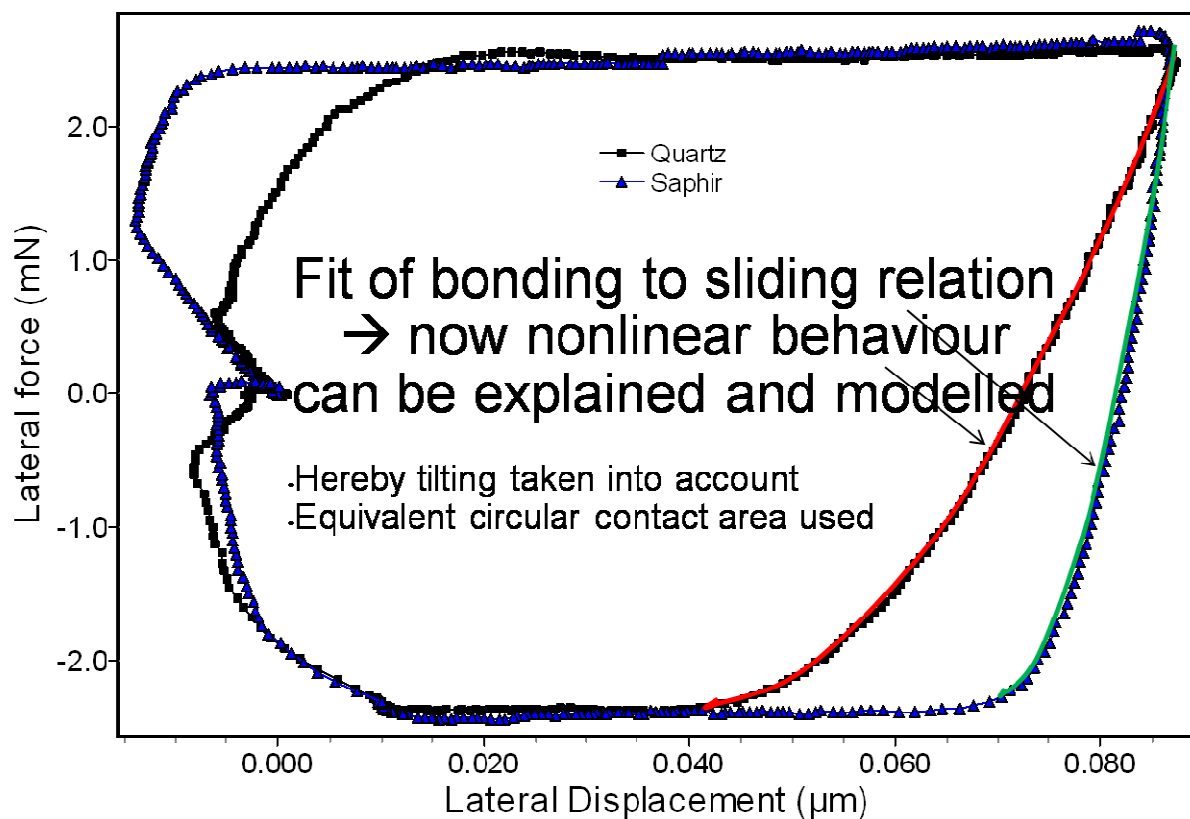


Figure 3: Two-fold contact area of partially bonded indenter fitted to the experimental lateral loading curve.

## HYPOTHETICAL APPLICATION: AN EXAMPLE

Let us assume that we possess a surface tester of the next generation allowing us to measure all stiffnesses given above. At first, we might like to compare  $S_3$  and  $S_4$ . They would be equal only in the complete isotropic case. So, we could determine the “amount” of anisotropy of the surface of any sample **locally** by simply comparing  $S_3$  and  $S_4$ . The more they diverge, the higher the anisotropy. **There is also a solution for high anisotropy available directly from the author.**

The next step would be to build the quotient  $Q_6$  equal to  $S_2$  over  $S_1$ .

$$Q_6 = \frac{4\pi(1+\theta_i^2)(1+\theta_s^2)^2(E_i+E_s-E_s\nu_i^2-E_i\nu_s^2)(E_s\theta_s(1+\theta_s^2)(-1+\nu_i+2\nu_i^2)+E_i\theta_i(1+\theta_i^2)(-1+\nu_s+2\nu_s^2))}{(\theta_i(\theta_s+\theta_s^3)(3E_s(1+\theta_s^2)(1+\nu_i)(-1+2\nu_i)(E_s(1+\theta_s^2)(-1+\nu_i+2\nu_i^2)+E_i(1+\theta_i^2)(-1+\nu_s+2\nu_s^2))+3E_i(1+\theta_i^2)(1+\nu_s)(-1+2\nu_s)(E_s(1+\theta_s^2)(-1+\nu_i+2\nu_i^2)+E_i(1+\theta_i^2)(-1+\nu_s+2\nu_s^2))+\frac{1}{\theta_i^2\theta_s^2}(2(E_s\theta_s(1+\theta_s^2)(-1+\nu_i+2\nu_i^2)+E_i\theta_i(1+\theta_i^2)(-1+\nu_s+2\nu_s^2))(\theta_i(1+\theta_i^2)\text{Sech}[\pi\theta_s](\pi\theta_s(1+\theta_s^2)(E_i+E_s+E_s\nu_i+E_i\nu_s)\text{Cosh}[\pi\theta_s]-E_i(1+4\theta_s^2)(-1+\nu_s^2)\text{Sinh}[\pi\theta_s])-E_s(1+4\theta_i^2)\theta_s(1+\theta_s^2)(-1+\nu_i^2)\text{Tanh}[\pi\theta_i])))} \quad (9)$$

Figure 4 gives the dependency on the sample Poisson's ratio for the example of a diamond tip and a variety of sample Young's moduli.

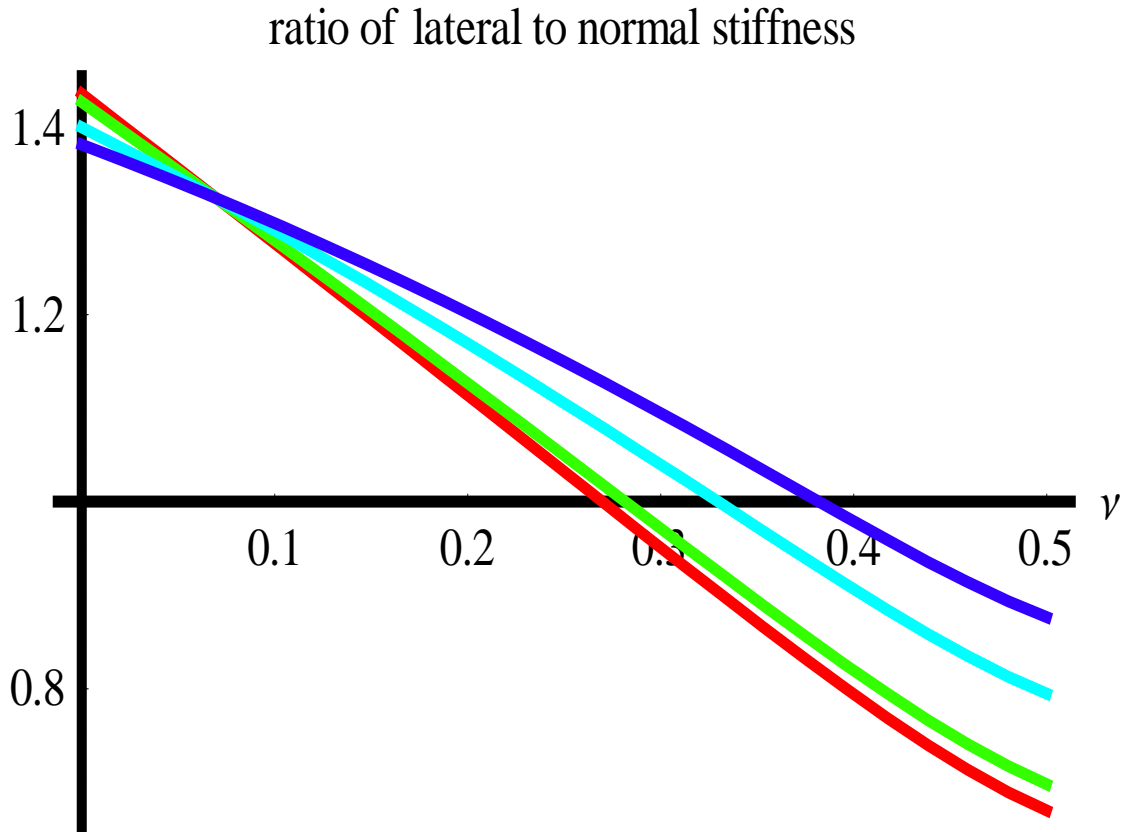


Fig. 4: Ratio of lateral to normal stiffness as defined in equation (9) as a function of the sample Poisson's ratio (red →  $E_s=10\text{GPa}$ , green →  $E_s=100\text{GPa}$ , light blue →  $E_s=500\text{GPa}$ , blue →  $E_s=1000\text{GPa}$ ).

As the material properties of the indenter should be known, equation (9) does not contain any other unknown material or contact parameters, except for the Young's modulus of the sample

Es. Thus, it is a very general expression allowing a rather significant connection of  $S_2/S_1$  with the unknown Poisson's ratio of the sample.

In a next step we determine the stiffness  $S_3$  and build the quotient  $Q=S_3/S_2$ .

$$Q = \frac{a \partial i \partial s (E_s (1 + \partial s^2) (-1 + \nu i + 2 \nu i^2) + E_i (1 + \partial i^2) (-1 + \nu s + 2 \nu s^2))}{E_s \partial s (1 + \partial s^2) (-1 + \nu i + 2 \nu i^2) + E_i \partial i (1 + \partial i^2) (-1 + \nu s + 2 \nu s^2)} \quad (10)$$

With this additional information we can establish the following results:

$$a = \frac{(4 B Q^2 \partial i - 2 B H_i Q S_1 \partial i^2 - 2 A Q S_1 \partial i \partial s + A H_i S_1^2 \partial i^2 \partial s - B H_i^2 S_1^2 \partial i^2 \partial s + 4 A Q S_1 \partial s^2 - A H_i S_1^2 \partial i \partial s^2 + B H_i^2 S_1^2 \partial i \partial s^2 + 2 A Q S_1 \partial i \partial s \nu s^2 - A H_i S_1^2 \partial i^2 \partial s \nu s^2 - 4 A Q S_1 \partial s^2 \nu s^2 + A H_i S_1^2 \partial i \partial s^2 \nu s^2 + 2 Q \partial i \sqrt{\partial i (4 A B S_1 (-2 Q + H_i S_1 \partial i) \partial s^2 (-1 + \nu s^2) + \partial i (B (-2 Q + H_i S_1 \partial s) - A S_1 \partial s (-1 + \nu s^2))^2) - H_i S_1 \partial s \sqrt{\partial i (4 A B S_1 (-2 Q + H_i S_1 \partial i) \partial s^2 (-1 + \nu s^2) + \partial i (B (-2 Q + H_i S_1 \partial s) - A S_1 \partial s (-1 + \nu s^2))^2) + H_i S_1 \partial s \sqrt{\partial i (4 A B S_1 (-2 Q + H_i S_1 \partial i) \partial s^2 (-1 + \nu s^2) + \partial i (B (-2 Q + H_i S_1 \partial s) - A S_1 \partial s (-1 + \nu s^2))^2)}}}{(2 \partial s (2 B Q \partial i - 2 B H_i S_1 \partial i^2 + A S_1 \partial i \partial s + B H_i S_1 \partial i \partial s - A S_1 \partial i \partial s \nu s^2 + \sqrt{\partial i (4 A B S_1 (-2 Q + H_i S_1 \partial i) \partial s^2 (-1 + \nu s^2) + \partial i (B (-2 Q + H_i S_1 \partial s) - A S_1 \partial s (-1 + \nu s^2))^2}))} \quad (11)$$

$$E_s = \frac{1}{2 A (2 Q - H_i S_1 \partial i) \partial s} (-2 B Q \partial i + A S_1 \partial i \partial s + B H_i S_1 \partial i \partial s - A S_1 \partial i \partial s \nu s^2 + (\partial i (4 A B S_1 (-2 Q + H_i S_1 \partial i) \partial s^2 (-1 + \nu s^2) + \partial i (B (-2 Q + H_i S_1 \partial s) - A S_1 \partial s (-1 + \nu s^2))^2))^{1/2} \quad (12)$$

With the constants A, B and Hi given as:

$$A = (\nu i + 2 \nu i^2 - 1) * (1 + \partial s^2), \quad B = E_i (1 + \partial i^2) * (\nu s + 2 \nu s^2 - 1) \quad \text{and} \quad H_i = (1 - \nu i^2) / E_i.$$

The substitution of  $E_s$  from equation (12) and a from equation (11) in equation (9) now allows us a determination of the sample Poisson's ratio directly from the measurement without any approximation or estimation as necessary in the classical Oliver and Pharr method [1]. After that the contact radius  $a$  and the sample Young's modulus  $E_s$  can be obtained from (11) and (12).

This means, that just by measuring certain surface stiffnesses of the sample, it is not only possible to determine the Poisson's ratio directly, but also to measure the contact radius without the need of knowing the indenter geometry and calibration (so called area function) calibration).

However, by keeping the procedure of area function calibration and measuring also the other stiffnesses left out so far, one might extract even more material parameters like the intrinsic stresses as described by the author elsewhere [6].

The method can also be extended to layered materials. The complex math behind this problem however, requires the use of computers and thus, the author has developed a software package performing the necessary evaluations [7]. Unfortunately, there is currently no surface testing machine available for the combined measurement of the stiffnesses as described above. Thus, we only demonstrate the principle possibilities of the software in modeling a mixed contact situation for layered materials. As an example of combined tilting, lateral and normal loading we have investigated a spherical probe scratch test with linearly increasing normal load on a rough surface (two layers) which topography has been scanned before. The result is shown in the following video animation <http://www.siomec.de/downloads/020>. The reader should especially pay attention to the fact, that the partially dramatic change in the stress field is mainly caused by

the tilting moments and change in lateral loads due to the effect of surface inclination during the scratch over the rather rough surface.

## CONCLUSIONS

It has been demonstrated how multi-axial indentation techniques can be used to determine additional material stiffnesses together with the normal stiffness. This allows the extraction of more material parameters and the contact radius in a directly manner without the need of area function calibration or knowledge of the indenter geometry. In the hypothetical example given in the paper, three stiffnesses, namely normal, lateral and lateral load to tilting angle, have been used to determine contact radius, Poisson's ratio and Young's modulus directly. But even more can be achieved when all degrees of freedom of indenter movement are used in future surface testing machines.

## REFERENCES

- [1] B. N. Lucas, J. C. Hay, W.C. Oliver: Using multidimensional contact mechanics experiments to measure Poisson's ratio. *J. Mater. Res.* 19, 58 (2004).
- [2] W.C. Oliver and G.M. Pharr: An improved technique for determining hardness and elastic modulus using load and displacement sensing indentation experiments. *J. Mater. Res.* 7, 1564 (1992).
- [3] N. Schwarzer, Short Note: Some Basic Equations for the Next Generation of Surface Testers Solving the Problem of Pile-up, Sink-in and Making Area-Function-Calibration obsolete, JMR Special Focus Issue on "Indentation Methods in Advanced Materials Research", submitted July 2008.
- [4] V. I. Fabrikant, "Mixed Boundary Value Problems of Potential Theory and their Application in Engineering", Kluwer Academic Publishers, The Netherlands, 1991.
- [5] N. Schwarzer, „Short note on the potential use of a rotating indenter with respect to the next generation of nanoindenters”, *Int. J. Surface Science and Engineering*, Vol.1 2007 2/3, pp. 239-258.
- [6] N. Schwarzer, "Intrinsic stresses – Their influence on the yield strength and their measurement via nanoindentation", online archives of the Saxonian Institute of Surface Mechanics, [www.siomec.de/pub/2007/001](http://www.siomec.de/pub/2007/001).
- [7] FilmDoctor®, software for the evaluation of mechanical contact for homogeneous and layered materials, [www.siomec.de/FilmDoctor](http://www.siomec.de/FilmDoctor).